



This is a repository copy of *μ -Particle tracking velocimetry and computational fluid dynamics study of cell seeding within a 3D porous scaffold.*

White Rose Research Online URL for this paper:
<http://eprints.whiterose.ac.uk/120947/>

Version: Accepted Version

Article:

Marin, A.C., Grossi, T., Bianchi, E. et al. (2 more authors) (2017) μ -Particle tracking velocimetry and computational fluid dynamics study of cell seeding within a 3D porous scaffold. *Journal of the Mechanical Behavior of Biomedical Materials*, 75. pp. 463-469. ISSN 1751-6161

<https://doi.org/10.1016/j.jmbbm.2017.08.003>

Reuse

This article is distributed under the terms of the Creative Commons Attribution-NonCommercial-NoDerivs (CC BY-NC-ND) licence. This licence only allows you to download this work and share it with others as long as you credit the authors, but you can't change the article in any way or use it commercially. More information and the full terms of the licence here: <https://creativecommons.org/licenses/>

Takedown

If you consider content in White Rose Research Online to be in breach of UK law, please notify us by emailing eprints@whiterose.ac.uk including the URL of the record and the reason for the withdrawal request.

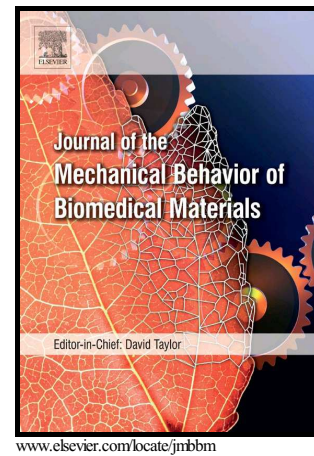


eprints@whiterose.ac.uk
<https://eprints.whiterose.ac.uk/>

Author's Accepted Manuscript

μ -Particle Tracking Velocimetry and Computational Fluid Dynamics study of cell seeding within a 3D porous scaffold

A. Campos Marin, T. Grossi, E. Bianchi, G. Dubini, D. Lacroix



PII: S1751-6161(17)30334-X
DOI: <http://dx.doi.org/10.1016/j.jmbbm.2017.08.003>
Reference: JMBBM2447

To appear in: *Journal of the Mechanical Behavior of Biomedical Materials*

Received date: 10 March 2017
Revised date: 25 July 2017
Accepted date: 2 August 2017

Cite this article as: A. Campos Marin, T. Grossi, E. Bianchi, G. Dubini and D. Lacroix, μ -Particle Tracking Velocimetry and Computational Fluid Dynamics study of cell seeding within a 3D porous scaffold, *Journal of the Mechanical Behavior of Biomedical Materials*, <http://dx.doi.org/10.1016/j.jmbbm.2017.08.003>

This is a PDF file of an unedited manuscript that has been accepted for publication. As a service to our customers we are providing this early version of the manuscript. The manuscript will undergo copyediting, typesetting, and review of the resulting galley proof before it is published in its final citable form. Please note that during the production process errors may be discovered which could affect the content, and all legal disclaimers that apply to the journal pertain.

μ -Particle Tracking Velocimetry and Computational Fluid Dynamics study of cell seeding within a 3D porous scaffold

A. Campos Marin¹, T. Grossi², E. Bianchi², G. Dubini², D. Lacroix^{1*}

¹ Insigneo Institute for in silico Medicine, Department of Mechanical Engineering, University of Sheffield, UK

² Laboratory of Biological Structure Mechanics, Department of Chemistry, Materials and Chemical Engineering 'Giulio Natta', Politecnico di Milano, Italy

***Corresponding author:** Insigneo Institute for in silico Medicine, Dept. Mechanical Engineering, The University of Sheffield, Pam Liversidge Building, Mappin Street, S1 3JD Sheffield, United Kingdom. Phone: +44 (0)114 2220156. Email: D.Lacroix@sheffield.ac.uk

Abstract

Cell seeding of 3D scaffolds is a critical step in tissue engineering since the final tissue properties are related to the initial cell distribution and density within the scaffold unit. Perfusion systems can transport cells to the scaffold however; the fact that cells flow inside the scaffold pores does not guarantee cell deposition onto the scaffold substrate and cell attachment. The aim of this study was to investigate how fluid flow conditions modulate cell motion and deposition during perfusion. For such a purpose, a multiphase-based computational fluid dynamics (CFD) model was developed in conjunction with particle tracking velocimetry experiments (PTV) which for the first time were applied to observe cell seeding inside a 3D scaffold. CFD and PTV results showed the strong effect of gravity for lower flow rates leading to cell sedimentation and poor transport of cells to the scaffold. Higher flow rates help overcome the effect of gravity so more cells travelling inside the scaffold were found. Nonetheless, fluid flow drags cells along the fluid streamlines without intercepting the scaffold substrate. As a consequence, if cells do not deposit into the scaffold substrate, cell adhesion cannot occur. Therefore, cell-scaffold interception should be promoted and the present computational model which predicts the effect of gravity and fluid drag on cells trajectories could serve to optimise bioreactors and enhance cell seeding efficiency.

Keywords

Porous scaffold; Cell seeding; CFD; Cell tracking; Microfluidics

Introduction

Tissue growth and functionality in 3D scaffolds are strongly related to the initial spatial distribution and density of cells. It is crucial to achieve homogeneous cell distribution during cell seeding so that uniform tissue growth can be expected [1]. Furthermore, maximum cell seeding efficiency is essential since donor cells are limited. Moreover, sufficient cell density in the scaffold unit is required to promote extracellular matrix formation and cell proliferation [2].

Traditional static methods for cell seeding such as manual pipetting, where gravity-driven cell deposition occurs, generally result in irregular cell density with higher number of cells at the outer part. In addition, there is a lack of cell viability since nutrients and oxygen do not always reach the centre of the 3D structure [3]. As an alternative, different dynamic flow strategies have been presented such as spinner flasks [4], wavy-walled bioreactors [5], rotating vessels [6], compression force-induced suction techniques [7] and perfusion systems [8]. Among all these hydrodynamic-based strategies, perfusion seems the most promising solution to enhance mass transfer homogeneously inside the scaffold in comparison with the other approaches [3,9,10]. However, the fact that cells penetrate in all scaffold regions during perfusion does not necessarily imply cell deposition on scaffold substrate. Cell deposition from suspension flow during perfusion is a complex mechanism that is not well understood yet. It can involve inertial impaction, interception, sedimentation and London-van der Waals forces [11].

Particle Tracking Velocimetry (PTV) methods have been applied to study cell motion in physiological fluids such as blood flow. These methods follow a similar principle to the μ -particle image velocimetry (PIV) but instead cells are tracked individually in a Lagrangian manner along time and space. Lima et al. [12] used PTV in combination with confocal microscopy to analyse the dynamic flow behaviour of red blood cells (RBCs) in different channel depths by optical sectioning. They found an increase of lateral displacement of cells when moving away from the plane at the centre of the microchannel. Sugii et al. [13] explored blood rheology in microcirculation using a multiphase flow approach where two sets of colour filters obtain separate images from fluorescent labelled RBCs and tracer particles. Oshima and Oishi [14] followed a similar approach although, to obtain the motion of RBCs, the cell membrane was marked by attaching on the surface electrically fluorescent particles of 0.2 μ m diameter. In this way, the deformation and the movement of the cells could be captured as well as the velocity distribution of the corresponding surrounding flow. However, to the authors' knowledge, scaffold cell seeding under fluid flow has not yet been investigated with PTV methods.

On the other hand, computational methods have been used to study scaffold cell seeding under dynamic flow. Spencer et al. [15] developed a μ CT-based scaffold model to predict the local fluid flow as well as transport of species and cell adhesion. However, cells were modelled as suspension concentrations being unable to predict individual cell behaviour. A multiphase approach was used by Adebisi et al. [16] where cells, considered as particles, were tracked individually along time and space in a vacuum based bioreactor. Nevertheless, the scaffold microstructure was modelled as a continuous porous medium that obeys Darcy's law. As a consequence, the actual scaffold microporosity was not considered and therefore realistic cell-scaffold interactions could not be investigated. A similar multiphase

approach was applied by Olivares and Lacroix [17], but instead scaffold geometry was digitally reconstructed with μ -Computed Tomography (CT) methods. A perfusion seeding system was simulated and good agreement in cell distribution inside the scaffold was found between computational and experimental results. Nevertheless, the influence of fluid flow conditions on cell motion and cell deposition onto scaffold substrate was not elucidated. In addition, it is noteworthy that none of these studies validated their predictions of cell motion dynamics with PTV experimental tests.

The aim of the present study is to investigate how fluid flow conditions modulate cell motion and deposition during dynamic seeding. The understanding and prediction of cell transport to scaffold substrate under fluid flow is essential for the optimization of bioreactors and the enhancement of seeding efficiency. For such a purpose, a multiphase-based CFD model is developed in conjunction with PTV experiments. A perfusion system is used to promote the transport of cells to the scaffold. In addition, a porous permeable scaffold with 100% interconnectivity is selected to enhance the delivery of cells inside the scaffold. To the authors' knowledge, this is the first time that dynamic cell seeding is captured inside the scaffold by performing PTV experiments. Moreover, these experimental data are used to formulate the computational multiphase model intended to predict cell transport during seeding.

Methods

PTV methods

Cell culture and labelling

MG63 cells were cultured in T-flasks under standard culture conditions at 37 °C and 5% CO₂ in an atmosphere of 99 % humidity. The culture medium was compounded by DMEM (Dulbecco's Modified Eagle Medium, Sigma D5671) supplemented with 1 mM sodium pyruvate, 10 mM HEPES buffer, 100 U/mL penicillin, 0.1 mg/mL streptomycin, 2 mM glutamine and 10% FBS (Fetal Bovine Serum). Media was refreshed every 48 hours and when confluency was reached, cells were trypsinized prior to the experiment.

Cells were labelled with orange CMTMR fluorescent dye (Life Technologies) using 10 μ M concentration in serum free medium. Cells were incubated for 45 min. Then, cells were centrifuged to remove the cell tracker working solution. Labelled cells were resuspended in culture media before the experiments. The final cell concentration for each experimental trial was 1×10^6 cells/mL.

Scaffold

A commercial Polycaprolactone scaffold from 3D Biotek (New Jersey, USA) was selected for this study (see Figure 1.a and b). The scaffold has a regular porous microstructure formed by layers of cylindrical fibres with 300 μ m diameter and 300 μ m distance between fibres. It has six layers with an offset of 90 degrees in the orientation of the fibres from layer-to-layer. In addition, there is a distance of 300 μ m among alternative layers. The scaffold has a

cylindrical shape with 5 mm diameter and 1.5 mm height. See more details about the scaffold design and manufacturing in Campos and Lacroix [18].

Microfluidic system configuration

The cylindrical scaffold was trimmed to fit inside a rectangular micro-channel to allow optical access inside porous microstructure during the PTV experiments. The micro-chamber was made of Polydimethylsiloxane (PDMS) with the following dimensions; 3x1x40 mm³. The depth of field of the tracking system permitted to focus the working plane within the first layer of pores that consisted of a series of vertical and horizontal fibres arranged in 3D (see Figure 1). The chamber was mounted on a surface glass by plasma-activated bonding.

A syringe pump (Harvard Apparatus PhD 2000) was connected to the micro-chamber to infuse the cells suspended in media. A time dependent flow pattern using a programmable syringe pump (NE-500, New Era Pump Systems, Farmingdale, NY, US) was selected. At the beginning a 300 µl/min flow rate was selected to carry cells to the scaffold to avoid cell sedimentation in the channel. Then, the flow rate was changed from 90 to 50 µl/min every 0.125 s. Above 50 µl/min cells were maintained in suspension so that cells could be observed inside the scaffold. Below 90 µl/min the camera frame rate was able to track cells along time and space.

Cell tracking procedure

The microfluidic chamber was placed on top of an inverted Olympus IX71 microscope stage with 10X optics magnification. A Nd:YAG laser with 532 nm of wavelength (TSI Incorporated, Minneapolis, USA) was used to excite the labelled cells in suspension. Single laser pulses were synchronised with a camera (Power View 4M, 2048 x 2048 pixels) to capture the reflected light from the cells in single frame images with a frequency of 14.5 Hz. Recorded images were imported to ImageJ where manual tracking was carried out using the plugin MTrackJ based on the bright centroid criteria.

It is noteworthy that due to the optics and the size of the tracer particles, out-of-focus cells within a specific depth could contribute to the cell tracking. This depth is commonly known as depth of correlation (DOC) and for this setup it is ~50 µm which was calculated using equation 1 proposed by [19]:

$$\text{DOC} = 2 \left[\frac{1 - \sqrt{\varepsilon}}{\sqrt{\varepsilon}} \left(f^{\#2} d_p^2 + \frac{5.95(M+1)^2 \lambda^2 f^{\#4}}{M^2} \right) \right]^{1/2} \quad (1)$$

where, magnification, $M = 10$; wavelength of the light emitted by the particles, $\lambda = 0.532$ µm; diameter of the particles, $d_p = 10$ µm; threshold value to determine the contribution of a particle to the measured velocity, $\varepsilon = 0.01$ and focal number, $f^{\#}$ is calculated by [20]:

$$f^{\#} = \frac{1}{2} \left[\left(\frac{n_o}{NA} \right)^2 - 1 \right]^{1/2} \quad (2)$$

where n_o , refractive index = 1 and numerical aperture, $NA = 0.3$.

Computational methods

μCT-based mesh generation

The trimmed scaffold was scanned using μCT (Skyscan1172, Materialise, Belgium) and digitally reconstructed with Simpleware (Synopsys, USA) (see details in Campos Marin et al. [21]). The micro-channel where the μCT-reconstructed scaffold was placed was generated using ICEM (ANSYS Inc., Canonsburg, PA, USA) as seen in Figure 1.c and d. The fluid domain was meshed with 4 million tetrahedral elements as explained in Campos Marin et al. [21].

Continuous phase modelling

The fluid phase represented the culture medium which was considered as an incompressible Newtonian fluid with a viscosity of 0.001 Pa·s and a density of 1000 kg/m³. The fluid phase was solved by the continuity and Navier-Stokes momentum equations. Transient laminar flow was simulated with a time-dependent flow rate; during the first 10 s the inlet flow rate was 300 μl/min and then it changed periodically between 50 to 90 μl/min every 0.125 s during 5 s. Zero pressure outlet and no-slip wall condition were applied.

Discrete phase modelling

Cells were modelled as a discrete phase of inert microsphere particles with 10 μm diameter. The discrete phase model of Fluent Ansys 15.0 tracks the particles along the previously calculated continuous phase in a Lagrangian formulation. Only one-way coupling was considered between both phases so the fluid phase could only affect the discrete phase. The trajectory of the discrete phase was calculated by integrating the force balance acting on the particle as shown in Equation 3 where the particle inertia is equal to the sum of the forces acting on the particle.

$$m_p \frac{dv_p}{dt} = \sum_{i=0}^n \vec{F}_i \quad (3)$$

$$\frac{du_p}{dt} = \frac{18\eta}{\rho_p d_p^2} \frac{C_d Re}{24} (u - u_p) + \frac{g(\rho_p - \rho)}{\rho_p} \quad (4)$$

The first term on the right of equation 4 is the drag force where η is the fluid dynamic viscosity, ρ is the fluid density, ρ_p is the density of the particle, d_p is the diameter of the particle, Re is the relative Reynolds number and C_d is an empirical drag coefficient factor for spherical particles [22]. The second term considers the effect due to the relative density between the discrete and the continuous phase. The density of cells was assumed to be greater than the density of the fluid phase, with a value of 1130 kg/m³ as suggested in the literature [23,24].

Stokes number (Stk) is a measurement of the tendency of a particle to deviate from the fluid streamline. Stk defines the ratio between the particle time scale versus the flow time scale as seen in equation 5:

$$\text{Stk} = \frac{\rho_p D_p^2 U}{18\mu D_{\text{obstacle}}} \quad (5)$$

where D_p is the diameter of the cell, D_{obstacle} is the fibre diameter and U is an average velocity of the fluid, thus D_{obstacle}/U defines the characteristic flow time. In this study Stk is $\ll 1$ which suggests that cells will follow the fluid streamlines.

Cells were injected using the surface injection method at the beginning of the simulations when the flow rate was 300 $\mu\text{l}/\text{min}$. One cell was injected per mesh element face at the inlet boundary. The inlet face presents 1,000 surface elements so four injections were required to inject a total of 4,000 cells in the fluid domain. Cells were injected with zero initial velocity and they were trapped as soon as they intercepted any wall boundary in the model.

Results

Cell transport to the scaffold

Below 50 $\mu\text{l}/\text{min}$ no cells are observed travelling inside the scaffold. Cells deposit on the bottom of the channel due to sedimentation. Higher flow rates attenuate the effect of gravity and increase the transport of cells to the scaffold (see Figure 2). This was also found computationally as seen in Figure 3. In the computational model, 300 cells were injected at the inlet boundary and the same flow rates applied for the PTV were investigated. For 20 $\mu\text{l}/\text{min}$, all cells sediment at the bottom of the channel before reaching the scaffold position; for 50 $\mu\text{l}/\text{min}$ some cells reach the scaffold position and 264 cells sediment before reaching the outlet of the channel; for 90 $\mu\text{l}/\text{min}$ more cells arrive to the scaffold position and 166 cells sediment before the channel outlet; for 180 $\mu\text{l}/\text{min}$ more cells than for 90 $\mu\text{l}/\text{min}$ reach the scaffold and 78 cells sediment in the channel before the outlet boundary (see Table 1).

Cell transport inside the scaffold (PTV)

The manual tracking performed using the plugin MTrackJ from ImageJ shows that cells mainly follow fluid streamlines. No cell adhesion was observed. Fluid streamlines seem preferable channels for cells to travel inside the scaffold as seen in Figure 4; a repeated number of cells pass by the same fluid streamline. In term of cells velocity, it can be seen that in region 1 shown in Figure 5 the velocities of cells are lower and then they increase in region 2 where cells travel towards the first pore. In region 3, where the first pore is found, cells decrease their velocity and then they move either to the left pore or the right one. More cells travel to the right pore as this pore is bigger yielding an irregular distribution of cells during seeding. The measured velocities of cells in that region are between 50 and 100 $\mu\text{m}/\text{s}$. However, this range of velocities differs significantly when moving to a different region inside the same scaffold with velocities up to 10 times higher (see Figure 6.a).

Cell transport inside the scaffold (PTV vs. CFD)

The CFD and PTV results agree on the fact that cells travel along the fluid streamlines inside the scaffold. In the computational model, only 3% of the cells injected intercept the scaffold

substrate during the simulation; particles are either deposited on the channel due to sedimentation or travel through the scaffold without intercepting it following the fluid streamlines. Even though CFD results agree well with the PTV experiments on cell path, they do not agree in terms of velocity values. Velocity values found in the CFD simulations can be from two to ten times higher than the values found in the PTV experiments. However, the CFD results also capture the significant increment of cell velocities from region to region with values up to ten times higher (see Figure 6.b).

Discussion

Transport of cells to the scaffold

Cells trajectory from the inlet of the channel to the scaffold entrance was found to be dependent on the inlet flow rate. Fluid drag becomes more dominant than gravity for higher flow rates which benefits the transport of cells to the scaffold. On the other hand, too low flow rates lead to cell sedimentation before arriving to the scaffold due to the strong effect of gravity. These findings show the key role of gravity during cell seeding and therefore it was included in the calculation of cells trajectory in the CFD model. In fact, cell density in the computational model was defined higher than the density of the culture media which was considered as water. Few studies in literature have attempted to measure the density of cells finding that values for cells such as human lung cancer cells (H1650), mouse lymphoblastic leukemia (L1210) or yeast cells are slightly higher than culture media (1000 kg/m^3) [23,24]. By accounting for this density difference between cells and culture media, the model could predict cell sedimentation with regard to the inlet flow rate selected. Both the experiments and the computational model agreed on the fact that for the micro-channel used in this study, flow rates below $50 \mu\text{L}/\text{min}$ are detrimental for maintaining cells in suspension and higher flow rates should be applied. However, too high flow rates could imply undesired shear stress which eventually could lead to the detachment of cells already adhered to the scaffold [25]. Moreover, excessive shear stress can induce integrin-initiated cytoskeletal deformation triggering unexpected cell response [26].

Transport of cells inside the scaffold

Inside the scaffold, cells mainly followed the fluid streamlines as suggested by the *Stk* calculation. Cell-scaffold interception was not observed during the tracking experiments due to the streamlines which did not drag cells towards the scaffold substrate preventing cell adhesion. Fluid drag seems to be the main driving force on cell motion inside the scaffold for flow rates higher than $50 \mu\text{L}/\text{min}$. Other physical factors such as van der Waals forces, Brownian motion or electrostatic forces seem hardly overcome the drag force and deviate cells from the fluid streamlines. However, a better insight into the interaction between the fluid flow and cell motion should be obtained by combining tracer particles and labelled cells in the working fluid simultaneously. Unfortunately, this strategy normally requires more than one filter to separate the fluorescence from labelled cells and tracer particles.

It is noteworthy that experimental conditions were not the most suitable for cell attachment since the scaffold surface was not treated to promote cell adhesion. The experiments were not performed under controlled temperature and humidity conditions and no scaffold sterilization was performed. However, cells do not impact the fibres due to the strong effect of the fluid flow on cell motion and, in the absence of any cell-scaffold interception, no chemical signalling for cell adhesion would occur, even under the most adequate biochemical seeding conditions. Nevertheless, a sensitivity analysis where the biochemical conditions are controlled would provide a deeper insight into the actual effect of the fluid drag force over other forces. In the computational model, cells were set to attach as soon as they impacted on the scaffold wall. This is not a realistic condition since a complex chain of events are involved in cell adhesion phenomena. However, if cells do not contact with the scaffold surface they will never adhere. So by knowing the number of cells that are intercepted on the scaffold wall in the computational model, the probability of cell attachment during experiments can be predicted.

The CFD results agree with the PTV experiments on the fact that cells follow the fluid streamlines due to the strong effect of fluid drag. In fact, a low percentage of cells contacting the scaffold substrate was found in the computational model; cells were either lost in the channel due to sedimentation or mainly travelled through the scaffold without touching it. Moreover, both techniques captured 10 times higher velocities when moving from one region to another within the scaffold. Even though both methods agree that gravity and fluid drag are key modulators of cell transport during cell seeding, significant differences were found in terms of cell velocity magnitude. It is noteworthy that the DOC is 100 μm so cells moving perpendicular to the focus plane along that depth can be observed during cell tracking. Thus, out-of-plane cells captured in the images can mislead cell velocity measurements since the observed cell path can be merely the projection of an out of plane trajectory. This limitation could be addressed by using calibration methods for PTV applications such as the one presented by Winer et al. [27] where the particle z-position is correlated to its apparent diameter.

Furthermore, the fact that a manual method for cell tracking was used could also contribute to the differences found between the velocities reported by PTV and CFD. However, the development of automatic tracking algorithms was out of the scope of this study. Pinho et al. [28] proposed an automatic method able to compute multiple trajectories in a time effective manner and compared it to the manual tracking method used in the present study and they did not find significant differences. Hence, manual tracking was considered accurate enough for the purpose of this study. Another reason for the disagreement between the PTV and CFD in terms of cells velocity magnitude can be the difficulty of recreating the exact geometrical boundary conditions in the CFD model. The real location of the scaffold due to manual fitting with respect to the channel walls is unknown and therefore it could be possible to find gaps which can potentially affect fluid dynamics inside the scaffold and cell motion. Larger gaps between the scaffold and the channel wall will have less resistance to flow than the scaffold pores so lower fluid and cell velocities could be expected inside the scaffold. It is noteworthy that the CFD model does not account for cell-to-cell interactions. This effect becomes more significant when cell density increases so there is more probability of cell collision deviating cells from their path and reducing their velocity leading to cell sedimentation or cell impaction on scaffold. The volume fraction

ratio of cells in the fluid domain selected for the CFD model was low enough that cell interactions could be neglected. However it could not be matched to the one of the PTV experiments due to an increase of computational cost when adding more cells in the model. Consequently, the high density of cells in the PTV experiments and therefore possible cell-to-cell interactions could be another reason why cells velocity calculated in the PTV experiments is lower than in the CFD results. In addition to this, the initial spatial distribution of cells during the injection could affect cell collisions. In the experiments, all cells enter in the micro-channel from the tube where they are compacted and high level of cell-to-cell interactions is expected. On the other hand in the CFD, cells are evenly distributed at the inlet face during the injection process preventing cell collision.

Nonetheless, more PTV experiments on the same scaffold are necessary to gain statistical significance. Unfortunately, the working fluid with labelled cells stained the scaffold which became too bright complicating thereby the optical cell tracking process. Despite this limitation, the findings of the present study elucidate the importance of the selection of the flow rate during seeding which influences the driving mechanisms: fluid drag and force due to gravity. Previous computational models for cell seeding did not consider the effect of gravity in cells trajectory [16,29]. Herein, it was shown that the inclusion of gravity leads to more realistic predictions where cell sedimentation and poor cell transport properties can be identified. The present computational model can help to design and optimise bioreactors to ensure cell transport to the scaffold. In addition, this study shows that different bioreactor configurations from perfusion should be proposed to promote cell-scaffold interception at the scaffold surface. For instance, the combination of perfusion with the rotation of the bioreactor or scaffold could enhance cell impaction onto the scaffold substrate [30]. This idea was implemented in the study of Melchels et al. [31] to analyse the seeding performance in a scaffold with regular pore network similar to the one used in the present study. A homogeneous cell distribution was found showing the benefit of this type of configuration for seeding. Another approach was followed by Papadimitropoulos et al. [32] who included a collagen network as filling material in a regular open scaffold to increase surface area. As a result, cell entrapment was increased in comparison to another scaffold sample where no collagen network was added.

Conclusions

The combination of regular permeable scaffolds with perfusion systems can enhance the transfer of cells inside the scaffold during seeding. However, this does not necessarily imply cell deposition on scaffold substrate and therefore cell adhesion. The aim of this study was to investigate the transport of cells inside a 3D scaffold during perfusion. To the authors' knowledge, this is the first time that cell seeding is observed and quantified inside a 3D porous scaffold by performing PTV experiments. Furthermore, these data served to formulate and validate a CFD model for scaffold cell seeding. The CFD model predicted the dominant role of fluid drag in cell transport for higher flow rates whereas force due to gravity overcomes fluid drag for lower flow rates. Furthermore, strong fluid drag drives cells along fluid streamlines avoiding cell-scaffold interception and cell attachment. The interception of cells with the scaffold substrate should be promoted and the present

computational model can help researchers design and optimise fluid-based bioreactors for such purpose. In spite of the good predictions of the computational model for the trajectory of cells, experiments using devices for tracking 3D displacements should be carried out to gain better insight into the cell transport phenomena and fully validate the CFD model.

Acknowledgements

The present study was funded by the European Research Council (258321) and the European Society of Biomechanics Mobility Award for young researchers. The authors want to acknowledge Dr. Gabriele Candiani for offering the opportunity to work in his research facilities and Chiara Diletta Malloggi for her technical support.

Conflict of interest

The authors declare that they have no conflict of interest.

References

- [1] A. Braccini, D. Wendt, C. Jaquierey, M. Jakob, M. Heberer, L. Kenins, A. Wodnar-Filipowicz, R. Quarto, I. Martin, Three-Dimensional Perfusion Culture of Human Bone Marrow Cells and Generation of Osteoinductive Grafts, *Stem Cells*. 23 (2005) 1066–1072. doi:10.1634/stemcells.2005-0002.
- [2] S. Saini, T.M. Wick, Concentric cylinder bioreactor for production of tissue engineered cartilage: Effect of seeding density and hydrodynamic loading on construct development, *Biotechnol. Prog.* 19 (2003) 510–521. doi:10.1021/bp0256519.
- [3] Y.L. Xiao, J. Riesle, C. a Van Blitterswijk, Static and dynamic fibroblast seeding and cultivation in porous PEO/PBT scaffolds., *J. Mater. Sci. Mater. Med.* 10 (1999) 773–7. doi:238489 [pii].
- [4] V.I. Sikavitsas, G.N. Bancroft, A.G. Mikos, Formation of three-dimensional cell/polymer constructs for bone tissue engineering in a spinner flask and a rotating wall vessel bioreactor, *J. Biomed. Mater. Res.* 62 (2002) 136–148. doi:10.1002/jbm.10150.
- [5] E.M. Bueno, B. Bilgen, G. a Barabino, Wavy-walled bioreactor supports increased cell proliferation and matrix deposition in engineered cartilage constructs., *Tissue Eng.* 11 (2005) 1699–1709. doi:10.1089/ten.2005.11.1699.
- [6] M. Nishi, R. Matsumoto, J. Dong, T. Uemura, Engineered bone tissue associated with

- vascularization utilizing a rotating wall vessel bioreactor, *J. Biomed. Mater. Res. Part A*. 101A (2013) 421–427. doi:10.1002/jbm.a.34340.
- [7] J. Xie, Y. Jung, S.H. Kim, Y.H. Kim, T. Matsuda, New technique of seeding chondrocytes into microporous poly (L-lactide-co- ϵ -caprolactone) sponge by cyclic compression force-induced suction, *Tissue Eng.* 12 (2006) 1811–1820.
- [8] F. Zhao, R. Chella, T. Ma, Effects of Shear Stress on 3-D Human Mesenchymal Stem Cell Construct Development in a Perfusion Bioreactor System : Experiments and Hydrodynamic Modeling, 96 (2007) 584–595. doi:10.1002/bit.
- [9] J.F. Alvarez-Barreto, S.M. Linehan, R.L. Shambaugh, V.I. Sikavitsas, Flow perfusion improves seeding of tissue engineering scaffolds with different architectures, *Ann. Biomed. Eng.* 35 (2007) 429–442. doi:10.1007/s10439-006-9244-z.
- [10] D. Wendt, a. Marsano, M. Jakob, M. Heberer, I. Martin, Oscillating perfusion of cell suspensions through three-dimensional scaffolds enhances cell seeding efficiency and uniformity, *Biotechnol. Bioeng.* 84 (2003) 205–214. doi:10.1002/bit.10759.
- [11] Y. Li, T. Ma, D. a. Kniss, L.C. Lasky, S.T. Yang, Effects of filtration seeding on cell density, spatial distribution, and proliferation in nonwoven fibrous matrices, *Biotechnol. Prog.* 17 (2001) 935–944. doi:10.1021/bp0100878.
- [12] R. Lima, T. Ishikawa, Y. Imai, M. Takeda, S. Wada, T. Yamaguchi, Measurement of individual red blood cell motions under high hematocrit conditions using a confocal micro-PTV system., *Ann. Biomed. Eng.* 37 (2009) 1546–59. doi:10.1007/s10439-009-9732-z.
- [13] Y. Sugii, R. Okuda, K. Okamoto, H. Madarame, Velocity measurement of both red blood cells and plasma of in vitro blood flow using high-speed micro PIV technique, *Meas. Sci. Technol.* 16 (2005) 1126–1130. doi:10.1088/0957-0233/16/5/011.
- [14] M. Oshima, M. Oishi, Continuous and Simultaneous Measurement of Micro Multiphase Flow Using confocal Micro-Particle Image Velocimetry (Micro-PIV) 3. Measurement for Droplet Formation, 4th Micro and Nano Flows Conference (MNF2014), London , (2014) 7–10.
- [15] T.J. Spencer, L. a. Hidalgo-Bastida, S.H. Cartmell, I. Halliday, C.M. Care, In silico multi-scale model of transport and dynamic seeding in a bone tissue engineering perfusion bioreactor, *Biotechnol. Bioeng.* 110 (2013) 1221–1230. doi:10.1002/bit.24777.
- [16] A.A. Adebisi, M.E. Taslim, K.D. Crawford, The use of computational fluid dynamic models for the optimization of cell seeding processes, *Biomaterials.* 32 (2011) 8753–8770. doi:http://dx.doi.org/10.1016/j.biomaterials.2011.08.028.
- [17] A.L. Olivares, D. Lacroix, Simulation of cell seeding within a three-dimensional porous scaffold: a fluid-particle analysis, *Tissue Eng. Part C Methods.* 18 (2012) 624–631.
- [18] A. Campos Marin, D. Lacroix, The inter-sample structural variability of regular tissue-

- engineered scaffolds significantly affects the micromechanical local cell environment, *Interface Focus*. 5 (2015). doi:10.1098/rsfs.2014.0097.
- [19] M.G. Olsen, R.J. Adrian, Out-of-focus effects on particle image visibility and correlation in microscopic particle image velocimetry, *Exp. Fluids*. 29 (2000) S166–S174. doi:10.1007/s003480070018.
- [20] C.D. Meinhart, S.T. Wereley, The theory of diffraction-limited resolution in microparticle image velocimetry, *Meas. Sci. Technol.* 14 (2003) 1047–1053. doi:10.1088/0957-0233/14/7/320.
- [21] A. Campos Marin, T. Grossi, E. Bianchi, G. Dubini, D. Lacroix, 2D μ -Particle Image Velocimetry and Computational Fluid Dynamics Study Within a 3D Porous Scaffold, *Ann. Biomed. Eng.* (2016). doi:10.1007/s10439-016-1772-6.
- [22] S. Morsi, A. Alexander, An investigation of particle trajectories in two-phase flow systems, *J. Fluid Mech.* 55 (1972) 193–208. doi:10.1017/S0022112072001806.
- [23] A.K. Bryan, V.C. Hecht, W. Shen, K. Payer, W.H. Grover, S.R. Manalis, Measuring single cell mass, volume, and density with dual suspended microchannel resonators., *Lab Chip*. 14 (2014) 569–76. doi:10.1039/c3lc51022k.
- [24] Y. Zhao, H.S.S. Lai, G. Zhang, G.-B. Lee, W.J. Li, Rapid Determination of Cell Mass and Density using Digitally-Controlled Electric Field in a Microfluidic Chip, *Lab Chip*. (2014). doi:10.1039/C4LC00795F.
- [25] Z. Tang, Y. Akiyama, K. Itoga, J. Kobayashi, M. Yamato, T. Okano, Shear stress-dependent cell detachment from temperature-responsive cell culture surfaces in a microfluidic device, *Biomaterials*. 33 (2012) 7405–7411. doi:10.1016/j.biomaterials.2012.06.077.
- [26] R.J. McCoy, F.J. O'Brien, Influence of shear stress in perfusion bioreactor cultures for the development of three-dimensional bone tissue constructs: a review., *Tissue Eng. Part B. Rev.* 16 (2010) 587–601. doi:10.1089/ten.teb.2010.0370.
- [27] M.H. Winer, A. Ahmadi, K.C. Cheung, Lab on a Chip tracking method to microfluidic particle focusing †, (2014) 1443–1451. doi:10.1039/c3lc51352a.
- [28] D. Pinho, R. Lima, A.I. Pereira, F. Gayubo, Automatic tracking of labeled red blood cells in microchannels, *Int. J. Numer. Method. Biomed. Eng.* 29 (2013) 977–987. doi:10.1002/cnm.2526.
- [29] A.L. Olivares, D. Lacroix, Computational Modeling in Tissue Engineering, in: L. Geris (Ed.), Springer Berlin Heidelberg, Berlin, Heidelberg, 2013: pp. 107–126. doi:10.1007/8415_2012_136.
- [30] S. Haykal, M. Salna, Y. Zhou, P. Marcus, M. Fatehi, G. Frost, T. Machuca, S.O.P. Hofer, T.K. Waddell, Double-Chamber Rotating Bioreactor for Dynamic Perfusion Cell Seeding of Large-Segment Tracheal Allografts: Comparison to Conventional Static

Methods., Tissue Eng. Part C. Methods. 20 (2014) 1–12.
doi:10.1089/ten.TEC.2013.0627.

- [31] F.P.W. Melchels, A.M.C. Barradas, C. a van Blitterswijk, J. de Boer, J. Feijen, D.W. Grijpma, Effects of the architecture of tissue engineering scaffolds on cell seeding and culturing., *Acta Biomater.* 6 (2010) 4208–17. doi:10.1016/j.actbio.2010.06.012.
- [32] A. Papadimitropoulos, S.A. Riboldi, B. Tonnarelli, E. Piccinini, M.A. Woodruff, A collagen network phase improves cell seeding of open-pore structure scaffolds under perfusion, (2013) 183–191. doi:10.1002/term.

Figures

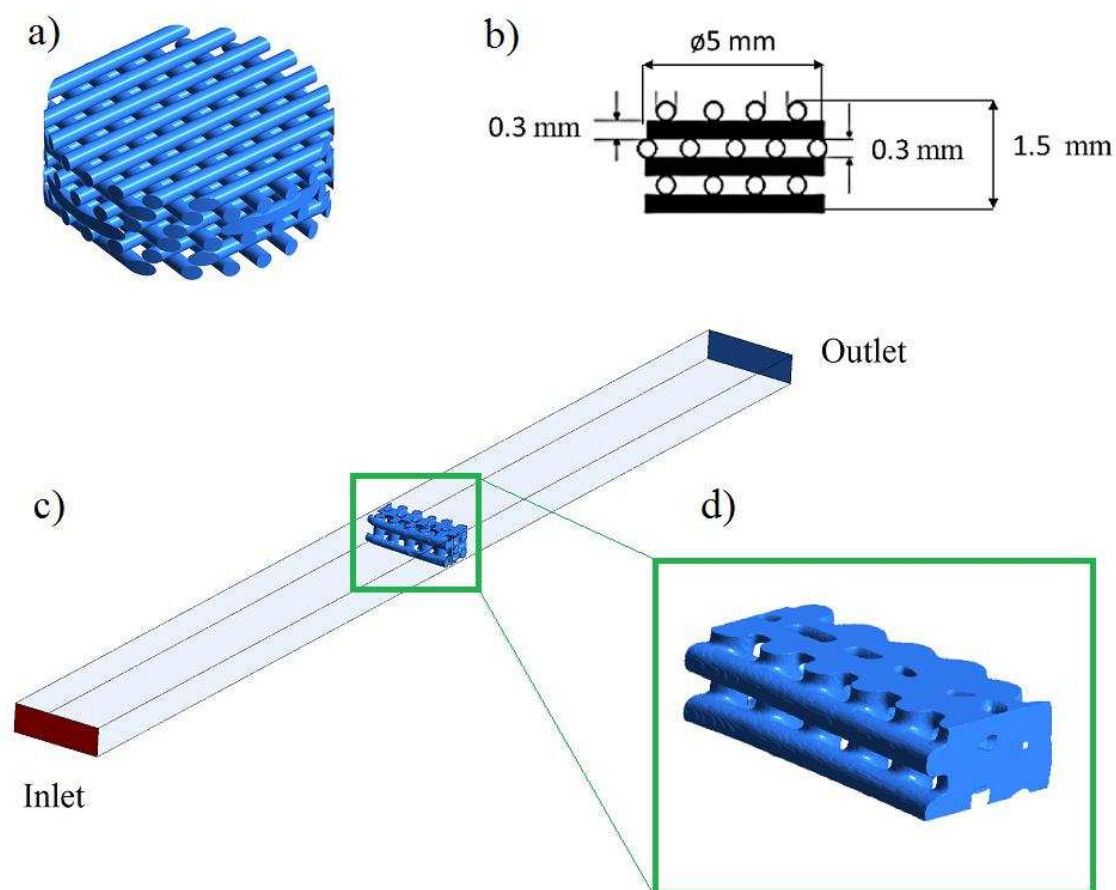


Figure 1 a) 3D CAD model of the 3D Biotek scaffold. b) Scaffold design specifications. c). CAD Micro-channel where the μ CT-based trimmed scaffold (d) was placed.

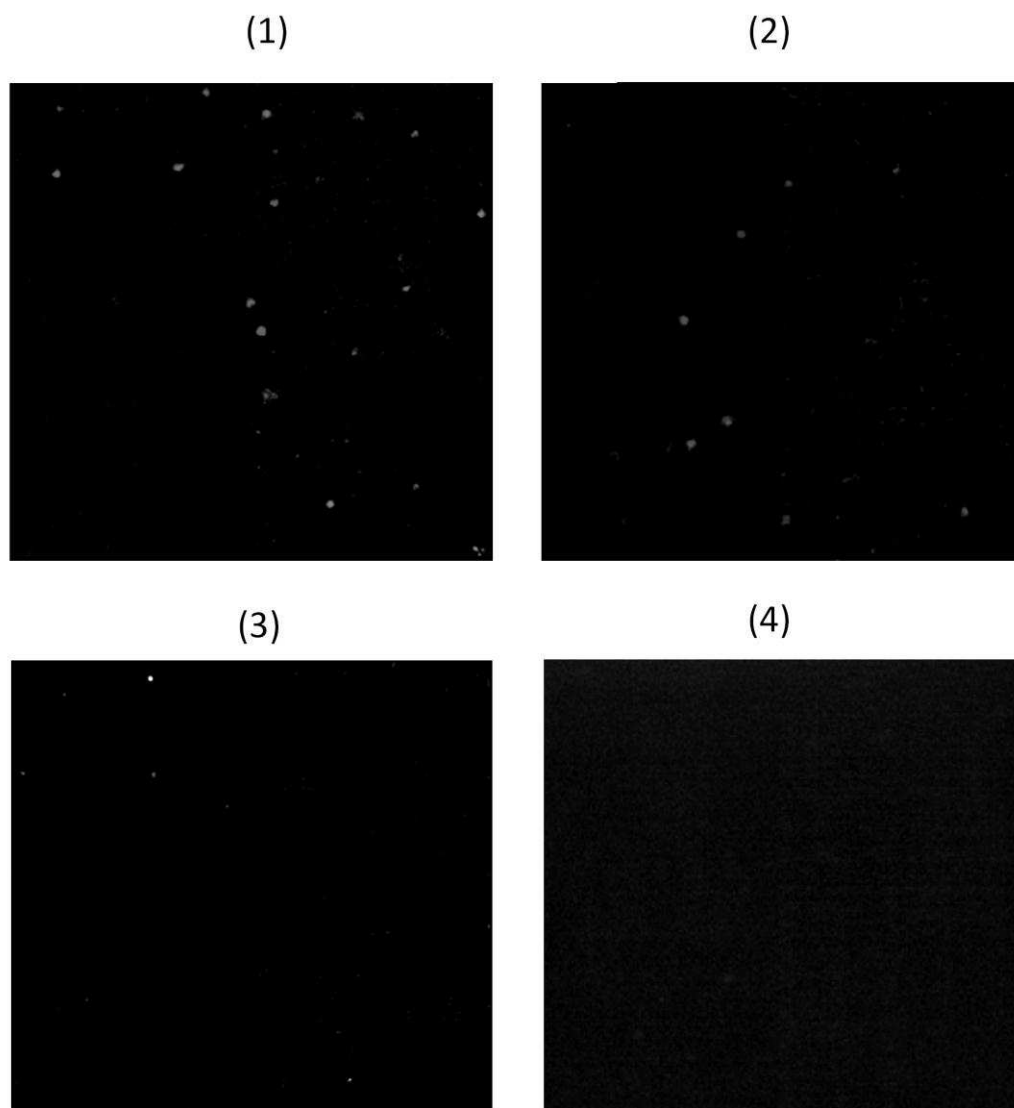


Figure 2 Labeled cells observed in the focus plane located at the scaffold location under difference flow rates. 1) For $180 \mu\text{l}/\text{min}$, ~ 18 cells are observed. 2) For $90 \mu\text{l}/\text{min}$, ~ 8 cells are observed. 3) For $50 \mu\text{l}/\text{min}$, 4 cells are observed. 4) For $20 \mu\text{l}/\text{min}$, no cells are observed.

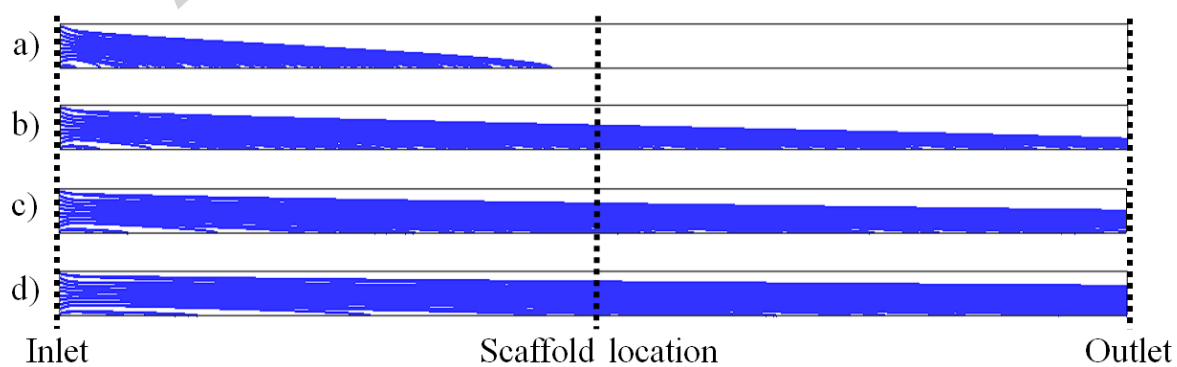


Figure 3 Blue lines represent the path of the cells injected to the micro-channel at the inlet under different flow rates. a) 20 $\mu\text{l}/\text{min}$ flow rate is applied and no cells reach the scaffold location. b) For 50 $\mu\text{l}/\text{min}$ some cells reach the scaffold location and also the outlet. c) 90 $\mu\text{l}/\text{min}$ flow rate brings more cells to the scaffold and the outlet. d) For 180 $\mu\text{l}/\text{min}$ cells trajectory is less affected by gravity than for the other flow rates leading to more cells crossing the scaffold and the outlet.

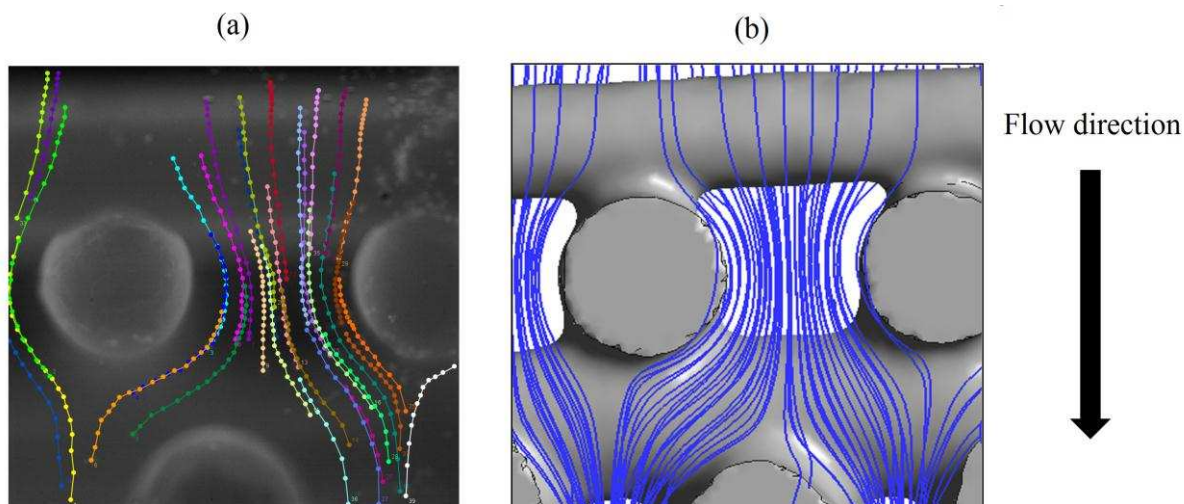


Figure 4 a) Cells trajectories in the PTV experiment. Each cell track is represented with a different color. Cells path in the tracking experiments are similar to the fluid streamlines predicted with CFD (b).

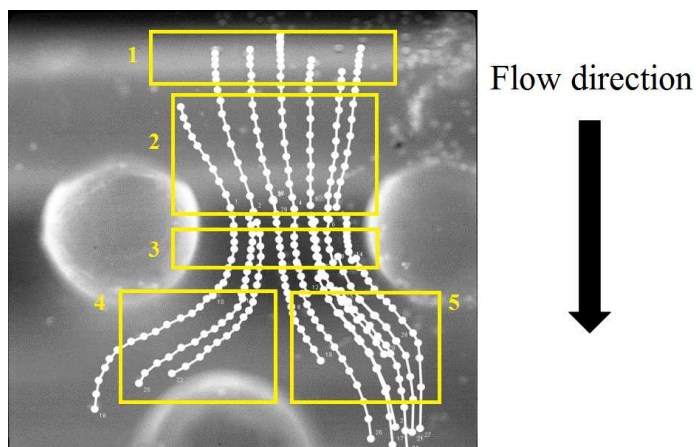


Figure 5 Cells trajectory in the PTV experiments. Each line represents one cell track where the white dots are the position of the cell along time. 1) Cells approach the horizontal fibre. 2) Cells travel towards the centre of the pore in the middle of the two vertical fibres. 3) Cells are in the centre of the pore and start deviating either towards the next left or right pore (4 and 5).

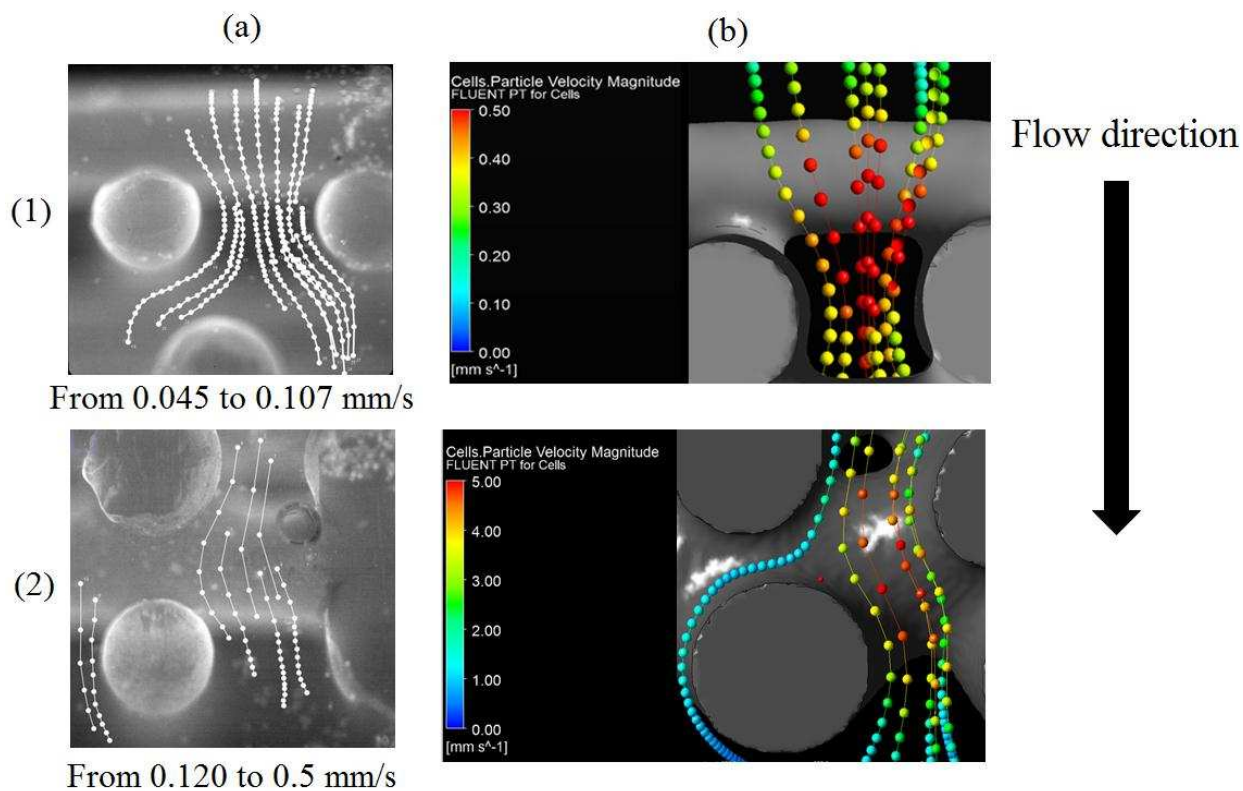


Figure 6 Cells path and velocity in two scaffold regions (1) and (2) using PTV (a) and CFD (b) methods.

Table 1 Particle tracking results from the CFD simulations. Number of cells that sediment or escape the micro-channel at the outlet from the 300 cells injected under different flow rates.

Flow rate [$\mu\text{l}/\text{min}$]	N ^o of sedimented cells	N ^o of escaped cells
20	300	0
50	264	36
90	166	131
180	78	222